© 2023 The Authors. *Orthopaedic Surgery* published by Tianjin Hospital and John Wiley & Sons Australia, Ltd.

RESEARCH ARTICLE

Long Noncoding RNA PCGEM1 Facilitates Tumor Growth and Metastasis of Osteosarcoma by Sponging miR-433-3p and Targeting OMA1

Jun Li, MM[1], Yuanjin Zhang, BSMed[1], Farui Sun, MM[1], Guofu Zhang, BSMed[1], Xi-an Pan, MM[1], Qian Zhou, MM[2]

Department of [1]Orthopedics and [2]Geriatrics, Huangshi Central Hospital, Huangshi, China

Objective: Osteosarcoma (OS) is regarded as one of the most common malignant bone tumors, mainly occurring in children and adolescents with high mortality. The dysregulation of lncRNAs is reported to regulate tumor development and be closely related to patient prognosis. Nevertheless, the role of long noncoding RNAs (lncRNAs) prostate-specific transcript 1 (PCGEM1) in OS remains uncharacterized. The current study aimed to explore the role of PCGEM1 in OS.

Methods: Reverse transcription-quantitative polymerase chain reaction (RT-qPCR) was performed to examine the expression of PCGEM1 in OS cell lines. CCK-8, colony formation, Transwell, and western blotting analyses were applied to measure OS cell viability, proliferation, migration, invasion, and epithelial-mesenchymal transition (EMT) after PCGEM1 downregulation. Nuclear-cytoplasmic fractionation, RNA pulldown, RNA immunoprecipitation (RIP), luciferase reporter assays were performed to verify the relationship among PCGEM1, miR-433-3p. and OMA1 in OS. The xenograft tumor models were established to evaluate the effect of PCGEM1 on tumor growth of OS.

Results: In this study, we discovered that PCGEM1 knockdown inhibited cell proliferation, migration, invasion and EMT in OS ($P < 0.05$). Additionally, PCGEM1 directly bound to miR-433-3p ($P < 0.01$). OMA1 was confirmed to be a target gene of miR-433-3p ($P < 0.05$), positively regulated by PCGEM1 but negatively regulated by miR-433-3p. Rescue assays further verified that overexpression of OMA1 reversed the PCGEM1 knockdown-mediated inhibitory effect on the malignant phenotype in OS cells ($P < 0.05$). Moreover, knockdown of PCGEM1 inhibited tumor growth and metastasis *in vivo* ($P < 0.05$).

Conclusions: Overall, PCGEM1 mediated tumor growth and metastasis of OS by sponging miR-433-3p and regulating OMA1, which might provide an innovative strategy for OS diagnosis or treatment.

Key words: miR-433-3p; OMA1; Osteosarcoma; PCGEM1

Introduction

Osteosarcoma (OS) is regarded as one of the most common malignant bone tumors, originating from mesenchymal cell lines and mainly occurring in children and adolescents.[1] The clinical symptoms of OS are pain, lumps, and claudication.[2,3] To date, OS is still a tumor with a high mortality rate in children and adolescents, but early diagnosis and timely treatment have greatly improved the survival rate of patients.[4,5] Therefore, it is of great urgency to reveal the molecular mechanisms involved in OS tumorigenesis and metastasis, identify novel biomarkers for early diagnosis, and develop effective therapies for OS treatment.

Long noncoding RNAs (lncRNAs) are longer than 200 nt that do not possess protein-coding functions due to the absence of an open reading frame of significant length.[6] Accumulated evidence has revealed that the dysregulation of lncRNAs is closely related to patient prognosis because of their regulatory roles in various pathophysiological processes.[7] Moreover, lncRNAs are involved in tumor physiology and pathology by regulating gene expression,[8] important

Address for correspondence Qian Zhou, MM, Department of Geriatrics, Huangshi Central Hospital, No. 141 Tianjin Avenue, Huangshigang District, Huangshi, 435000, Hubei, China; Email: zq20161015@163.com
Received 1 March 2022; accepted 8 December 2022

This is an open access article under the terms of the Creative Commons Attribution-NonCommercial-NoDerivs License, which permits use and distribution in any medium, provided the original work is properly cited, the use is non-commercial and no modifications or adaptations are made.

Open Access

Orthopaedic Surgery

to proliferation[9] and metastasis.[10] The lncRNA prostate cancer gene expression marker 1 (Prostate-specific transcript 1, PCGEM1) gene is located at chromosome 2q32.3, without protein-coding capacity.[11] In recent years, many studies have demonstrated key roles of of PCGEM1 in the initiation and development of cancers, such as renal carcinoma and endometrial cancer.[12,13] Through diverse functional mechanisms, PCGEM1 has a large effect on downstream genes and then regulates cancer cell proliferation, invasion and apoptosis.[14,15] PCGEM1 can influence other diseases, such as asthma and osteoarthritis.[16,17] More importantly, preclinical experiments and *in vitro* studies have shown the tremendous clinical potential of PCGEM1.[18,19] This literature demonstrates that PCGEM1 may be a potential target in cancer treatment, which inspired us to investigate the specific role and mechanism of PCGEM1 in OS.

MicroRNAs (miRNAs) can regulate the levels of target genes at the posttranscriptional level by binding with the 3′ untranslated regions (3'UTRs) of target genes.[20,21] MiR-10b-3p was reported to promote tumor growth and metastasis of esophageal squamous cell carcinoma by targeting TSGA10.[22] MiR-708 has been proven to act as a novel regulator of Hoxa9 in acute myeloid leukemia.[23] Recently, it was reported that miR-433-3p suppresses cell proliferation and invasion in esophageal squamous cell carcinoma by targeting GRB2.[24] Moreover, miR-433-3p promotes osteoblast differentiation by reducing DKK1 expression *via* the WNT/β-catenin pathway.[25] However, the knowledge about the function of miR-433-3p in OS still remains to be explored.

In this study, we hypothesized that: (i) PCGEM1 is differentially expressed in OS; (ii) PCGEM1 participates in OS cell proliferation, migration, invasion, and tumor growth in OS; and (iii) PCGEM1 functions as a "sponge" for miR-433-3p to affect the expression of downstream target. Therefore, this study aimed to: (i) investigate whether PCGEM1 plays an oncogenic role in OS progression; (ii) uncover the molecular mechanisms how PCGEM1 affects OS progression; and (iii) provide promising therapeutic molecular biomarkers for OS treatment.

Materials and Methods

Cell Lines

The OS cell lines (MG-63, U2OS, Saos2 and 143B) and human normal osteoblast cell line hFOB1.19 were purchased from the Chinese Academy of Science Cell Bank (Shanghai, China). All cells were cultured in Dulbecco's modified Eagle's medium (DMEM, Gibco, Bristol, RI, USA) containing 10% fetal bovine serum (FBS, Gibco, Bristol, RI, USA) in a humidified atmosphere with 5% CO_2 at 37°C.

Cell Transfection

MiR-433-3p mimics were used to overexpress miR-433-3p with NC mimics as a negative control. Short hairpin RNA (shRNA) targeting PCGEM1 (sh-PCGEM1#1/2) was used to knock down PCGEM1 with sh-NC as a negative control. Full-length OMA1 was inserted into pcDNA3.1 to overexpress OMA1 with empty pcDNA3.1 as a control. Afterwards, Lipofectamine 3000 (Invitrogen, Austin, TX, USA) was applied to conduct cell transfection at 37°C with 40 nM MiR-433-3p mimics or NC mimics. The transfection efficiency was examined by RT-qPCR after 48 h.

Real-Time Reverse Transcription Polymerase Chain Reaction (RT-qPCR)

Total RNA was isolated from OS tissues, cells and xenograft tumors by TRIzol reagent (Invitrogen) and reverse transcribed into complementary DNA (cDNA) by M-MLV Reverse Transcriptase (Invitrogen). RT-qPCR was conducted using SYBR Premix Ex Taq II kit (Takara, Dalian, China) on an ABI Prism 7500 Real-Time PCR System (Applied Biosystems, Foster City, CA, USA) according to the manufacturer's instructions. GAPDH served as an internal control for PCGEM1 and mRNAs. For miRNA analysis, RT-qPCR was performed using the TaqMan miRNA Reverse Transcription Kit (4,366,596; Thermo Fisher Scientific, Waltham, MA, USA). U6 served as an internal control for miRNAs. The relative expression of target genes was calculated by the $2^{-\Delta\Delta Ct}$ method. Primer sequences used for RT-qPCR are listed in Table 1.

Cell Proliferation Assays

Cell proliferation was assessed using a Cell Counting Kit-8 kit (CCK-8; Dojindo Chemical Laboratory, Kumamoto, Japan) assay and colony formation assay. For the CCK-8 assay, cells (3×10^3/well) were seeded into 96-well plates

TABLE 1 Primer sequences used for RT-qPCR

Target	Primer sequences (5′–3′)
PCGEM1	F: CGATCATGATGGGCTCCTCG
	R: GTGCAGGGTCCGAGGT
MiR-433-3p	F: TCGGCAATCATGATGGGCTCCTC
	R: CTCAACTGGTGTCGTGGAGTC
miR-148a-3p	F: AGCAGTTCAGTGCACTACAG
	R: GCAGGGTCCGAGGTATTC
miR-129-5p	F: ACACTCCAGCTGGGCTTTTTGCGGTCTGG
	R: CTCAACTGGTGTCGTGGAGTCGG CAATTCAGTTGAGGCAAGCCC
MiR-152-3p	F: TCGGCAGGTCAGTGCATGACAGAA
	R: CTCAACTGGTGTCGTGGA
MiR-526b-5p:	F: TTTACATCCTAGCCTGTGATC
	R: CAGCAATGGATTTTAAGCCAAG
MiR-506-3p	F: ACACTCATAAGGCACCCTTC
	R: TCTACTCAGAAGGGGAGTAC
MiR-182-5p	F: TTAGGAACCCTCCTCTCTC
	R: ACTTTCGTTCTTGAGGAATG
PCCB	F: CTACGCATTTGCTGAGGCA
	R: GACATCATAGGCACCTCCA
OMA1	F: TTTCTGCCATTCAGCATCC
	R: CTTTCCGAGCATTCCGAAC
U6	F: GCTTCGGCAGCACATATACTAAAAT
	R: CGCTTCAGAATTTGCGTGTCAT
GAPDH	F: CTGGGCTACACTGAGCACC
	R: AAGTGG TCGTTGAGGGCAATG

with 100 μL DMEM containing 10% FBS. Approximately 10 μL CCK-8 solution was added to the plate at 0, 24, 48, and 72 h, followed by another 2 h of incubation. The absorbance was measured using a microplate reader (Scientific MultiskanMK3, Thermo Scientific, Waltham, MA, USA) at 450 nm. For the colony formation assay, the transfected cells (1000 cells/well) were seeded into 6-well plates. Cells were then cultured for 14 days at 37°C. Next, the cells were fixed in methanol, stained with 0.1% crystal violet for 30 minutes and imaged. The colonies were counted using an inverted microscope (Olympus, Tokyo, Japan).

Transwell Assay

Transwell chambers (8 mm, BD Biosciences, Swindon, UK) coated with or without Matrigel (40111ES08, Shanghai Yisheng Biotechnology, China) were used to assess cell invasion or migration. In short, cells (5×10^4) suspended in serum-free DMEM were added to the upper chambers coated with Matrigel. Then, 600 μL DMEM with 10% FBS was added to the bottom chamber in the 24-well plates. Then, both the upper and bottom chambers were incubated for 48 h at 37°C with 5% CO_2. The cells on the surface of the upper chamber were gently removed with a cotton swab. The invaded cells were collected, fixed with 10% formaldehyde, and stained with 0.2% crystal violet. The cells from five visual fields were counted under an inverted microscope (Tokyo, Japan). For cell migration detection, similar procedures were performed as above except that Matrigel was not used.

Western Blot Analysis

Total proteins were extracted from MG-63 and U2OS cells by using Protein Lysis Buffer (Beyotime, Shanghai, China) and quantified by BCA Protein Assay Kit (Beyotime, Shanghai, China). Then, cell lysates were isolated by 10% sodium dodecyl sulfate, polyacrylamide gel electrophoresis (SDS-PAGE) and transferred onto a polyvinylidene fluoride (PVDF) membrane (Millipore, Billerica, MA, USA). Afterwards, the membrane was blocked with defatted milk and incubated with primary antibodies overnight at 4°C and then incubated with the secondary antibody (ab205719; 1:5000, Abcam) at room temperature for 2 h after washing with phosphate-buffered saline (PBS). Finally, the blots were visualized by enhanced chemiluminescence Plus and analyzed by ImageJ software. Primary antibodies against E-cadherin (ab1416), N-cadherin (ab18203), vimentin (ab8978), OMA1 (ab154949) and GAPDH (ab9485) were purchased from Abcam (Cambridge, USA).

Nuclear-Cytoplasmic Fractionation

The subcellular localization of PCGEM1 in the cytoplasm or nucleus of MG-63 and U2OS cells was determined using a PARIS Kit (Life Technologies, Beverly, MA, USA). Briefly, MG-63 and U2OS cell pellets were resuspended in cold cell fractionation buffer and incubated on ice for 5 min. After centrifugation, the supernatant was harvested. GAPDH and U6 were utilized as controls in the cytoplasm and nucleus, respectively. The extracted RNAs were measured by RT-qPCR.

Bioinformatics Analysis and Luciferase Reporter Assay

The online tool starBase v2.0 (http://starbase.sysu.edu. cn/) was used to predict the target miRNAs of PCGEM1 and the target genes of miR-433-3p. The binding site between PCGEM1 and miR-433-3p was predicted from starBase (search category: low stringency of CLIP Data and two cancer types of Pan-cancer). The binding site between miR-433-3p and OMA1 was predicted from starBase (search category: 10 cancer types in Pan-cancer; Predicted Program: miRanda, PicTar and TargetScan).

The wild-type or mutant sequence of PCGEM1 or OMA1 3'UTR containing the putative binding site of miR-433-3p was subcloned into the pmirGLO vector (Promega Corporation, Madison, WI, USA) to generate the PCGEM1-Wt/Mut or OMA1 3'UTR-Wt/Mut reporter. All plasmids were synthesized by GenePharma (Shanghai, China) and transfected into OS cells using Lipofectamine 3000 (Invitrogen, Waltham, MA, USA) following the manufacturer's instructions.

RNA Pulldown Assay

PCGEM1 probe with biotin and control PCGEM1 probe without biotin were purchased from GenePharma (Shanghai, China) and incubated with the lysates of MG-63 and U2OS cells for 1 h, followed by pulldown by M-280 streptavidin magnetic beads (Invitrogen, Waltham, MA, USA) at 4°C overnight. The RNA attached to the beads was washed and extracted. The enrichment of miRNAs was detected by RT-qPCR.

RNA Immunoprecipitation (RIP) Assay

A Magna RNA immunoprecipitation (RIP) kit (Millipore, Billerica, MA, USA) was used in the RIP assay. MG-63 and U2OS cells were collected and lysed in RIPA lysis buffer. Then, magnetic beads containing Ago2 (Invitrogen, Waltham, MA, USA) or IgG antibody were added to the cell lysates. Input was the positive control, and anti-IgG was the negative control. Finally, RNA in immunoprecipitates was extracted using TRIzol and quantified by RT-qPCR.

Tumor Formation Assay in Nude Mice

All animal experiments were conducted in accordance with the guidelines for the Institutional Animal Care and Use of Laboratory Animals (8th Edition, 2011, National Research Council). A total of 20 athymic nude BALB/c mice (5 weeks old, 18–20 g) were purchased from Vital River Co., Ltd. (Beijing, China). For xenograft tumors, 5×10^6 U2OS cells stably transfected with sh-PCGEM1, or sh-NC vector were inoculated subcutaneously in the right flanks of BALB/c nude mice ($n = 5$ in each group). The mice were killed on day 21, and then tumors were resected, imaged, and weighed.

Tumor volumes were examined every 7 days and calculated by using the equation V (mm^3) = length × $width^2$/2. For the metastasis model, cells with different treatments were injected into the tail veins of BALB/c nude mice (n = 5 in each group).

Histological Examination

OS tumor specimens were fixed in 4% paraformaldehyde overnight and then embedded in paraffin. The tumor sections were incubated with the Ki-67 antibody (Calbiochem, Darmstadt, Germany) and OMA1 antibody with 1:50 dilution for 4 h. Visualization was achieved by using the 3, 3′-diaminobenzidine substrates (Dako, Glostrup, Denmark) followed by counterstaining with hematoxylin. The representative images were captured and the positive cells were quantified with Image J.

Statistical Analysis

Statistical analysis was conducted with SPSS 17.0 statistics software (IBM Corp., Armonk, NY, USA). Each experiment was performed at least three times, and data are shown as the mean ± standard deviation (SD). The differences between two groups or more than two groups were calculated by Student's t test or one-way ANOVA test. The value of $P < 0.05$ was statistically significant.

Results

Inhibition of PCGEM1 Suppresses Cell Proliferation, Migration, Invasion and EMT in OS

To understand the function and regulatory mechanism of PCGEM1 in OS, we examined the expression level of PCGEM1 in OS cells. RT-qPCR analysis showed that PCGEM1 expression was relatively higher in OS cell lines (MG-63, U2OS, Saos2 and 143B) than in the normal osteoblast cell line hFOB1.19 (*$P < 0.05$) (Fig. 1A). Since the expression of PCGEM1 had no significant change among these four cell lines, MG-63 and U2OS cells were randomly selected for subsequent functional experiments to explore the effects of PCGEM1 on OS cell function. As revealed in Fig. 1B, PCGEM1 expression was effectively knocked down in MG-63 and U2OS cells after transfection with sh-PCGEM1#1 or sh-PCGEM1#2 (*$P < 0.05$) (Fig. 1B). Based on the data from CCK-8 and colony formation assays, cell viability and colony formation ability in MG-63 and U2OS cells both decreased after PCGEM1 knockdown (*$P < 0.05$) (Fig. 1C,D), indicating that PCGEM1 knockdown inhibited OS cell proliferation. In addition, Transwell assays demonstrated that transfection of sh-PCGEM1#1 or #2 suppressed the migratory and invasive capacity of MG-63 and U2OS cells (*$P < 0.05$) (Fig. 1E,F). The EMT process plays a key role in cell migration and invasion. Herein, the levels of EMT markers, including E-cadherin and N-cadherin, were measured by western blot analysis. We discovered that inhibition of PCGEM1 upregulated the expression of E-cadherin but downregulated the expression of N-cadherin in MG-63 and U2OS cells (Fig. 1G). In conclusion, PCGEM1 might functionally facilitate the malignant phenotype of OS cells *in vitro*.

PCGEM1 Acts as a Molecular Sponge for miR-433-3p

We then investigated the molecular mechanism of PCGEM1 in OS. As presented in Fig. 2A, the majority of PCGEM1 was distributed in the cytoplasm of MG-63 and U2OS cells. It has been widely reported that lncRNAs in the cytoplasm can function as ceRNAs to release mRNA by acting as miRNA sponges in cancers.[26] Thus, we hypothesized that PCGEM1 may act as a ceRNA in OS. With the assistance of starBase (http://starbase.sysu.edu.cn), seven miRNAs with a binding site on PCGEM1 were predicted (screening conditions: low stringency of CLIP Data and two cancer types of Pan-cancer) (Fig. 2B). To select the miRNA interacting with PCGEM1 in OS, an RNA pulldown assay was conducted, and we found that only miR-433-3p was enriched in the PCGEM1 probe with biotin among these candidate miRNAs (**$P < 0.01$) (Fig. 2C). RT-qPCR revealed that the miR-433-3p level was lower in OS cells than in hFOB1.19 cells (*$P < 0.05$) (Fig. 2D). Additionally, miR-433-3p expression was significantly increased in PCGEM1 knockdown cells (*$P < 0.05$) (Fig. 2E). Subsequently, we overexpressed miR-433-3p by transfecting miR-433-3p mimics into MG-63 and U2OS cells (*$P < 0.05$) (Fig, 2F). A luciferase reporter assay demonstrated that miR-433-3p mimics suppressed the luciferase activity of vectors carrying the wild-type but not mutant PCGEM1 sequence (*$P < 0.05$) (Fig, 2G). Overall, PCGEM1 exerts a function as a miR-433-3p sponge in OS cells.

MiR-433-3p Directly Targets OMA1

Next, we aimed to identify the target gene of miR-433-3p. StarBase was used to predict the candidate genes. Through filtration (conditions: 10 cancer types in Pan-cancer; Predicted Program: miRanda, PicTar and TargetScan), PCCB and OMA1 were identified (Fig. 3A). As shown in Fig. 3B, OMA1 expression was upregulated in OS cells, while PCCB displayed no detectable change among these cells (*$P < 0.05$) (Fig. 3B). Additionally, RT-qPCR and western blot analyses indicated that miR-433-3p expression was negatively correlated with OMA1 expression, while PCGEM1 expression was positively associated with OMA1 expression in OS cells (*$P < 0.05$) (Fig. 3C,D). A luciferase reporter assay showed that the luciferase activity of the OMA1 3'UTR-Wt reporter was decreased by miR-433-3p overexpression (*$P < 0.05$) (Fig. 3E). RIP assays demonstrated that PCGEM1, miR-433-3p and OMA1 were all enriched in the Ago2 group compared to the IgG group, implying that these RNAs coexisted in the RNA-induced silencing complex (*$P < 0.05$) (Fig. 3F). All these data revealed that OMA1 was a direct target of miR-433-3p.

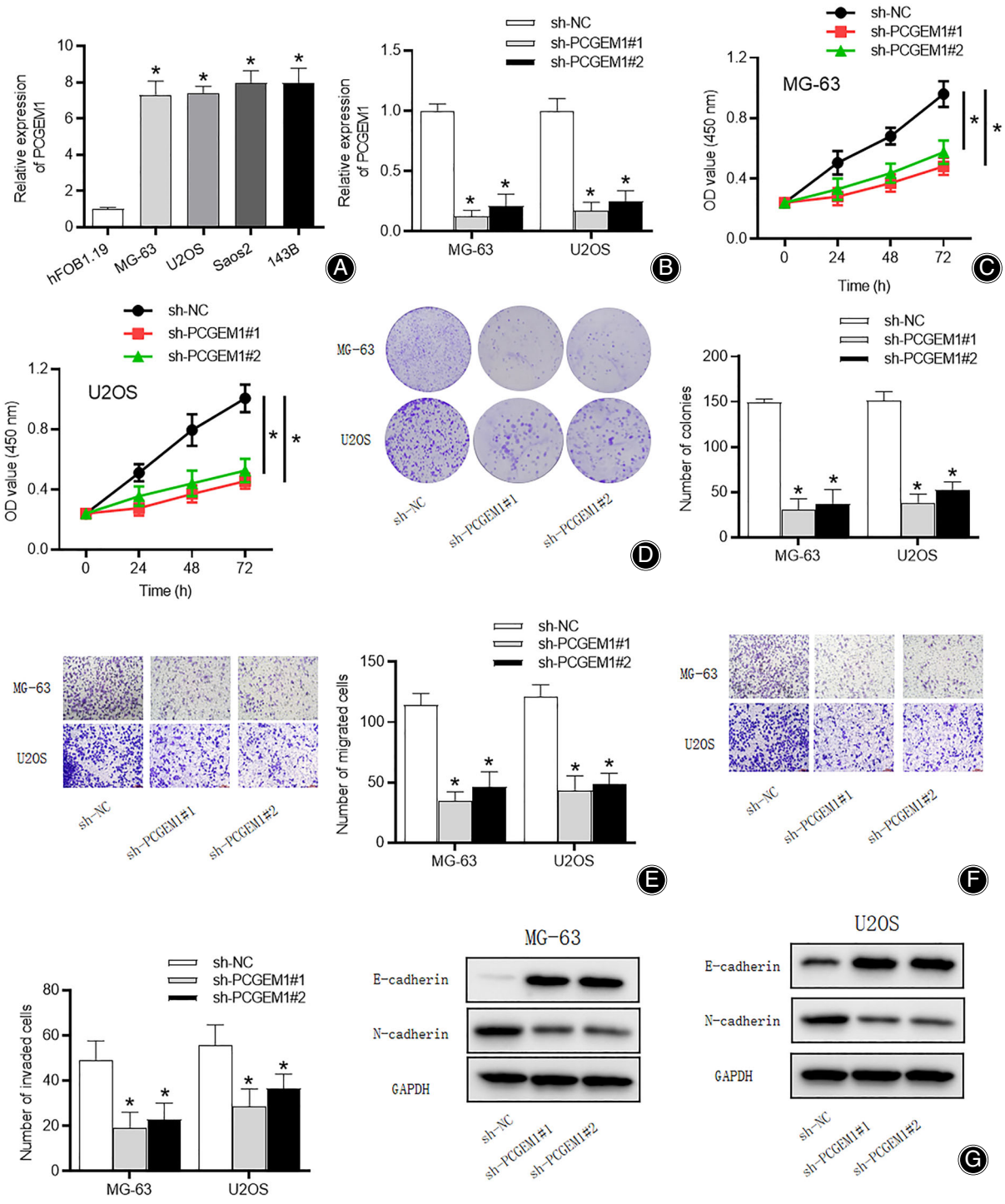

Fig. 1 Inhibition of PCGEM1 suppresses cell proliferation, migration, invasion and EMT in OS. (A) RT-qPCR analysis was used to determine the expression of PCGEM1 in OS cells (MG-63, U2OS, Saos2 and 143B) and hFOB1.19 cells. (B) The expression of PCGEM1 in MG-63 and U2OS cells transfected with sh-PCGEM1#1/2 was detected by RT-qPCR analysis. (C) The viability of MG-63 and U2OS cells after inhibition of PCGEM1 was evaluated by CCK-8 assay. (D) The proliferation of MG-63 and U2OS cells after knockdown of PCGEM1 was assessed by colony formation assays. (E) The migration and (F) invasion of MG-63 and U2OS cells after suppression of PCGEM1 were examined by Transwell assays. (G) Western blot analysis was performed to measure the protein levels of E-cadherin and N-cadherin in MG-63 and U2OS cells transfected with sh-PCGEM1#1/2. *$P < 0.05$

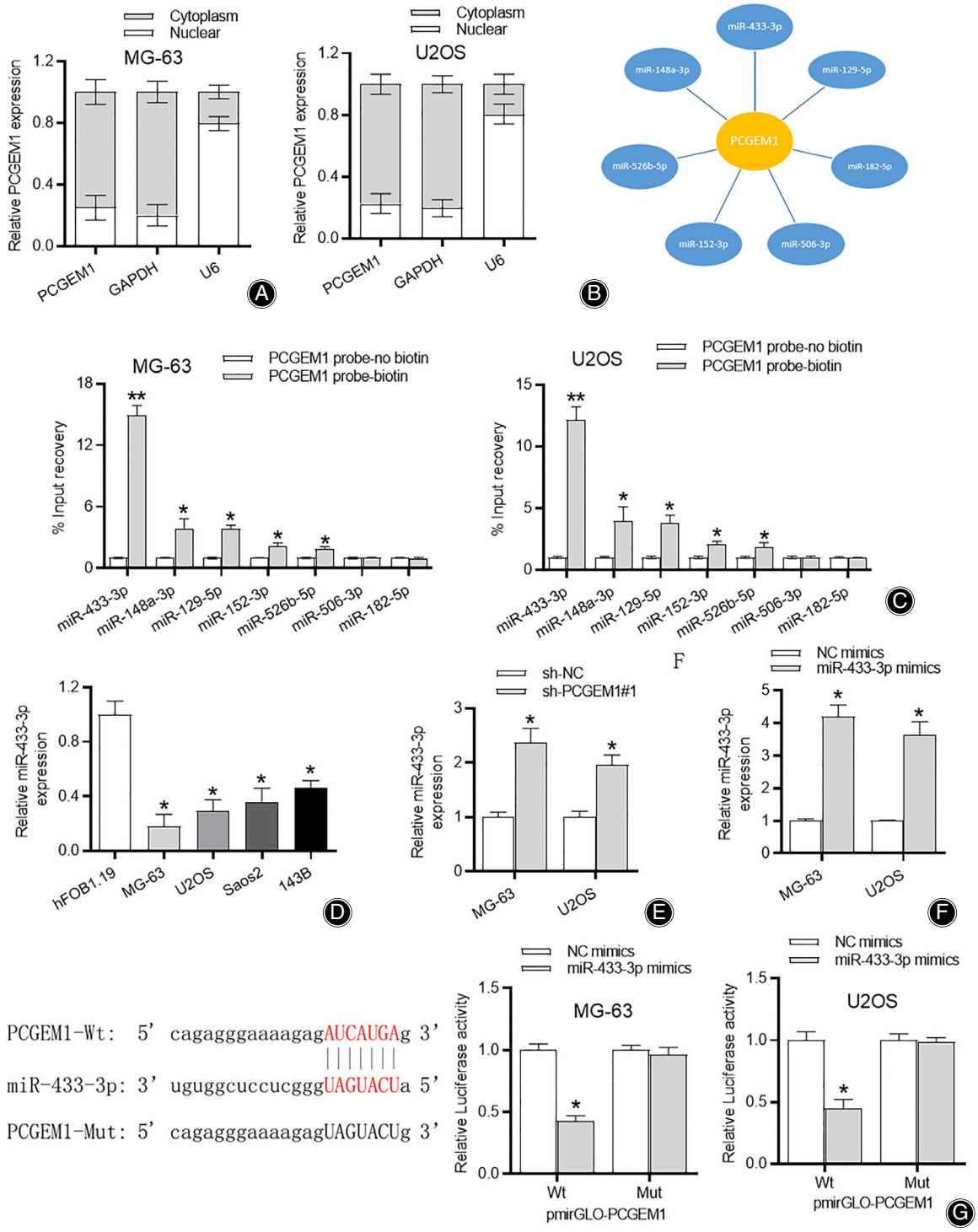

Fig. 2 PCGEM1 acts as a molecular sponge for miR-433-3p. (A) A nuclear-cytoplasmic fractionation assay was used to determine the subcellular localization of PCGEM1 in MG-63 and U2OS cells. (B) The starBase database predicted miRNAs binding to PCGEM1. (C) RNA pulldown assay showed the enrichment of miRNAs from the PCGEM1 probe. (D) RT-qPCR analysis was performed to determine the expression of miR-433-3p in OS cells (MG-63, U2OS, Saos2 and 143B) and hFOB1.19 cells. (E) The expression of miR-433-3p in MG-63 and U2OS cells transfected with sh-PCGEM1#1 was measured using RT-qPCR. (F) The expression of miR-433-3p in MG-63 and U2OS cells transfected with miR-433-3p mimics was determined by RT-qPCR. (G) The binding sequences were predicted by starBase, and a luciferase reporter assay was used to validate the interaction between PCGEM1 and miR-433-3p. * $P < 0.05$, ** $P < 0.01$

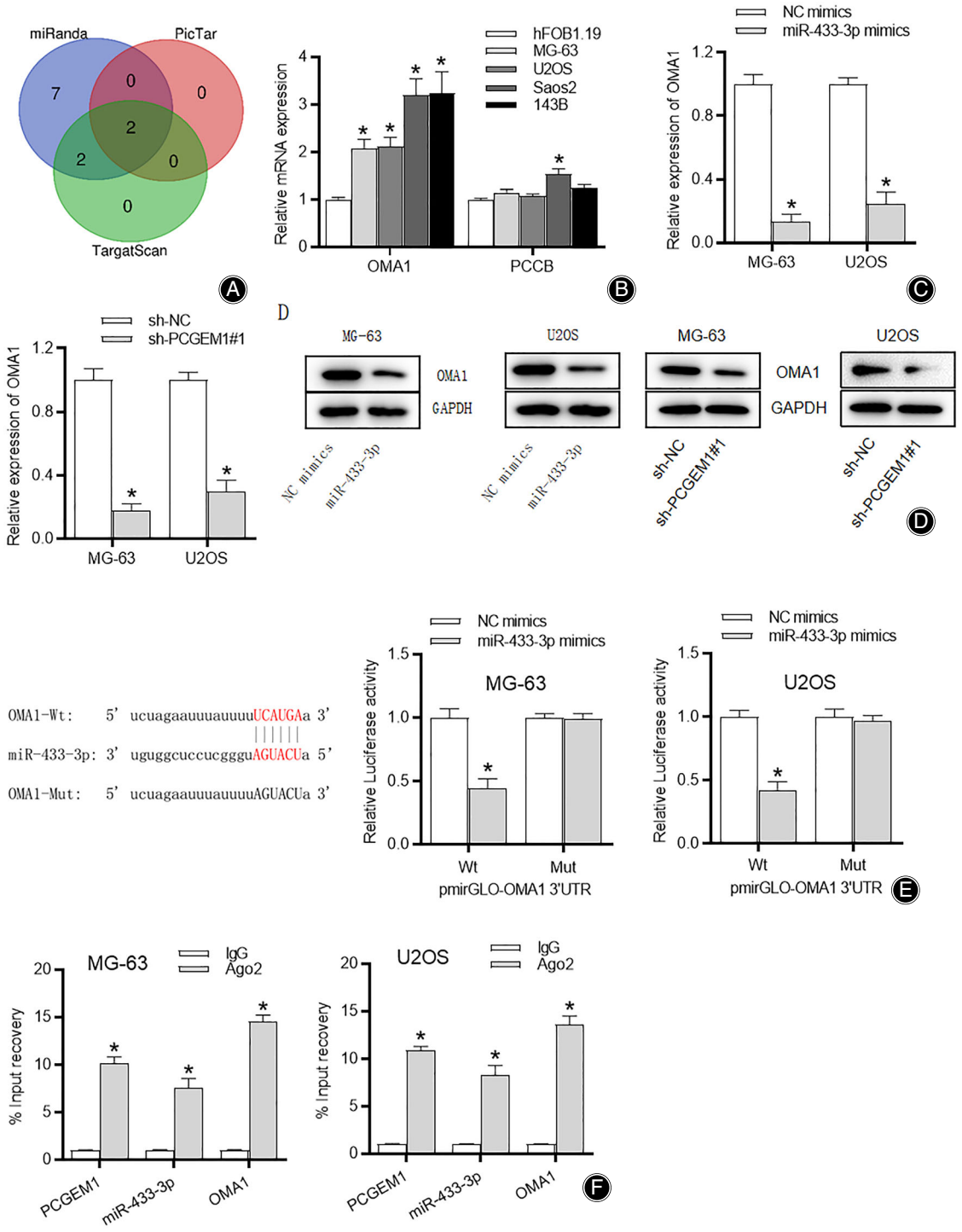

Fig. 3 MiR-433-3p directly targets OMA1. (A) The Venn diagram shows the potential target genes of miR-433-3p predicted by miRanda, PicTar and TargetScan. (B) The mRNA expression of PCCB and OMA1 in OS cells (MG-63, U2OS, Saos2 and 143B) and hFOB1.19 cells was analyzed by RT-qPCR. (C-D) RT-qPCR and western blot analyses were performed to examine the mRNA and protein levels of OMA1 in MG-63 and U2OS cells transfected with miR-433-3p mimics or sh-PCGEM1#1. (E) The binding site between miR-433-3p and the OMA1 3'UTR was predicted by starBase, and a luciferase reporter assay was conducted to verify the binding of miR-433-3p to the OMA1 3'UTR. (F) RIP assay was performed to examine the coexistence of PCGEM1, miR-433-3p and OMA1 in RISC. * $P < 0.05$

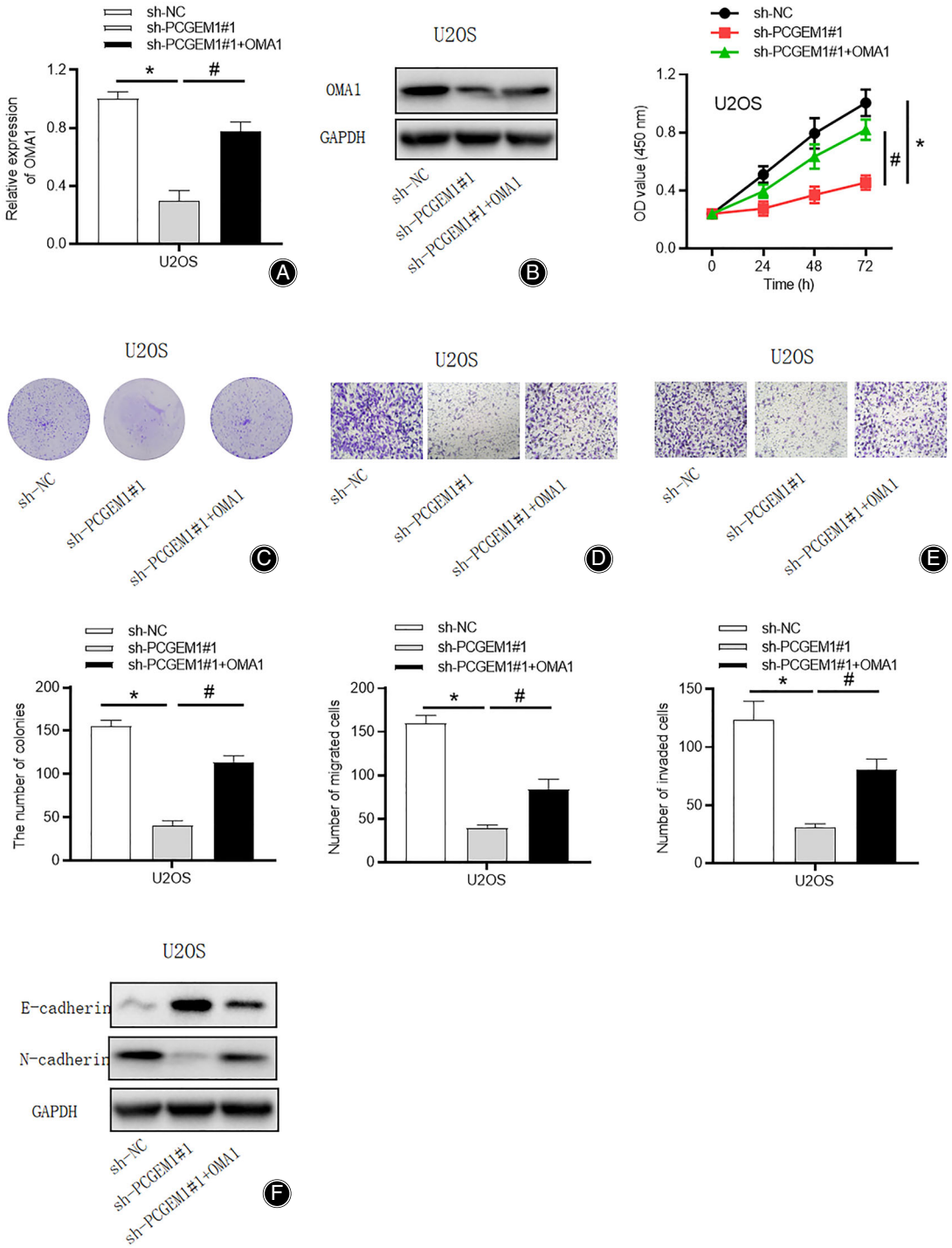

Fig. 4 Upregulation of OMA1 reverses the PCGEM1 knockdown-induced suppressive effect on the malignant phenotype in OS cells. (A) The overexpression efficiency of pcDNA3.1/OMA1 in MG-63 and U2OS cells was evaluated by RT-qPCR and western blot analyses. (B-C) Cell viability and proliferation were detected by CCK-8 and colony formation assays in MG-63 and U2OS cells after transfecting sh-NC, sh-PCGEM1#1 or sh-PCGEM1#1 + OMA1. (D-E) Cell migration and invasion were tested by Transwell assays in MG-63 and U2OS cells after transfecting sh-NC, sh-PCGEM1#1 or sh-PCGEM1#1 + OMA1. (F) Western blot analysis was used to determine the E-cadherin and N-cadherin levels in MG-63 and U2OS cells after transfecting sh-NC, sh-PCGEM1#1 or sh-PCGEM1#1 + OMA1. * $P < 0.05$ *vs*. the sh-NC group. # $P < 0.05$ *vs*. the sh-PCGEM1 group

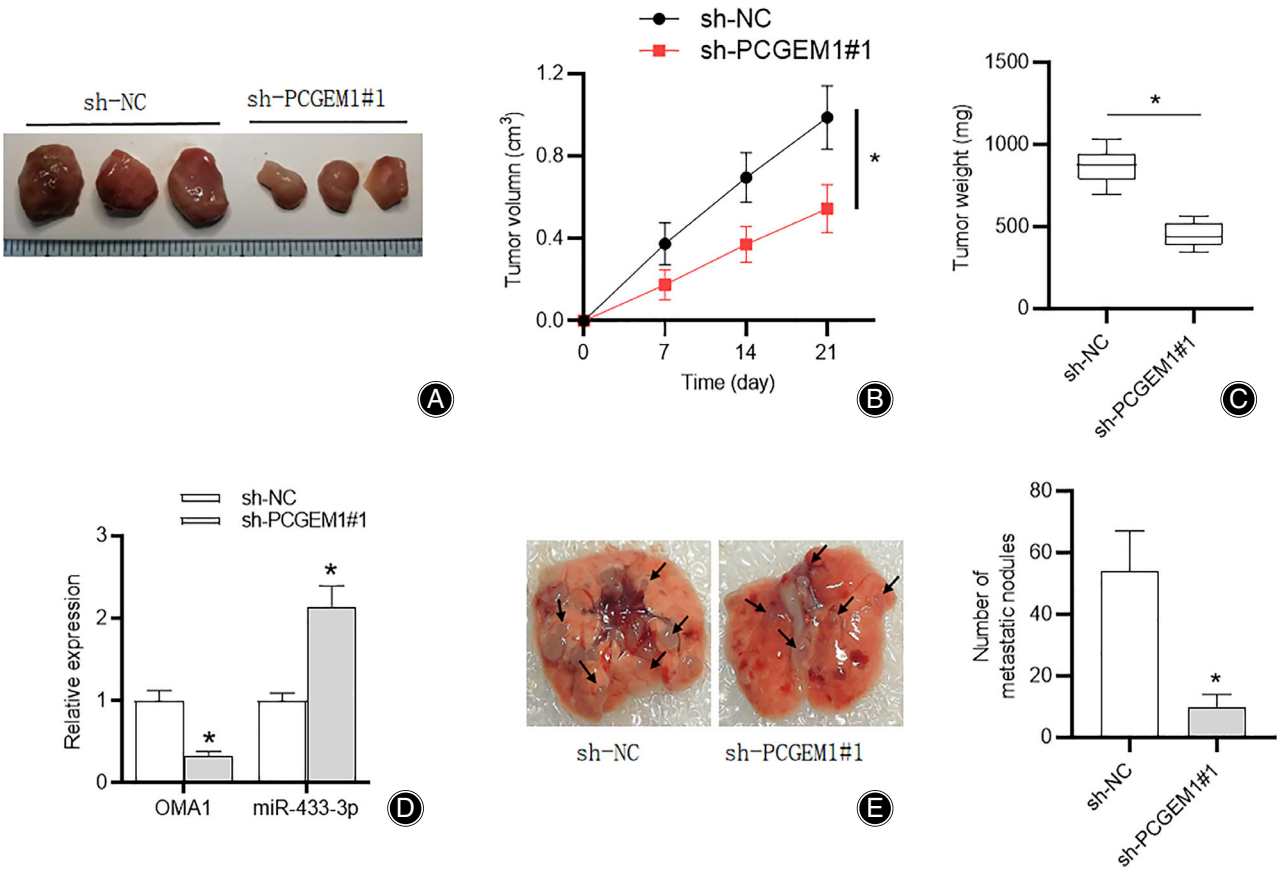

Fig. 5 Knockdown of PCGEM1 inhibits OS tumor growth and metastasis *in vivo*. (A) Representative images showing tumor xenografts in nude mice. (B) Tumor volume in nude mice (n = 5). (C) Tumor weight in nude mice (n = 5). (D) The expression of OMA1 and miR-433-3p in surgically removed tumor tissues. (E) Representative images and quantification of lung metastasis. * $P < 0.05$

Upregulation of OMA1 Reverses the PCGEM1 Knockdown-Induced Suppression Effect on the Malignant Phenotype of OS Cells

To validate the PCGEM1/miR-433-3p/OMA1 regulatory axis in OS, rescue assays were carried out. RT-qPCR and western blot analyses showed that the reduction in OMA1 mRNA and protein levels caused by PCGEM1 silencing was reversed by OMA1 overexpression ($^*P < 0.05$; $^{\#}P < 0.05$) (Fig. 4A). Then, CCK-8 and colony formation assays revealed that the suppressive effect of PCGEM1 knockdown on cell viability and proliferation was attenuated after cotransfection of sh-PCGEM1#1 and pcDNA3.1/OMA1 into U2OS cells ($^*P < 0.05$; $^{\#}P < 0.05$) (Fig, 4B,C). Transwell assays showed that OMA1 overexpression counteracted the inhibitory effect of PCGEM1 silencing on cell migration and invasion abilities ($^*P < 0.05$; $^{\#}P < 0.05$) (Fig. 4D,E). Furthermore, the increase in E-cadherin and the decrease in N-cadherin mediated by knockdown of PCGEM1 were restored after overexpression of OMA1 (Fig. 4F). To conclude, PCGEM1 promoted the malignant phenotype of OS cells by upregulating OMA1.

Knockdown of PCGEM1 Inhibits OS Tumor Growth and Metastasis in Vivo

We established a xenograft tumor model by injecting U2OS cells stably expressing sh-PCGEM1#1 or sh-NC to explore the role of PCGEM1 *in vivo*. As shown in Fig, 5A,B, tumors from the sh-PCGEM1#1 group had smaller size and weight than those from the control group ($^*P < 0.05$). As recorded weekly, mice in the sh-PCGEM1#1 group had tumors with a smaller volume than those in the sh-NC group ($^*P < 0.05$) (Fig. 5C). In addition, RT-qPCR was used to detect the expression of OMA1 and miR-433-3p in surgically removed tumor tissues. The results showed that knockdown of PCGEM1 downregulated OMA1 and upregulated miR-433-3p expression ($^*P < 0.05$) (Fig. 5D). To investigate the effect of PCGEM1 on tumor metastasis *in vivo*, cells with different treatments were separately injected into the tail veins of nude mice. The results revealed that lung metastasis in the sh-PCGEM1#1 group was alleviated ($^*P < 0.05$) (Fig. 5E). In summary, downregulation of PCGEM1 inhibited OS tumor growth and metastasis *in vivo*.

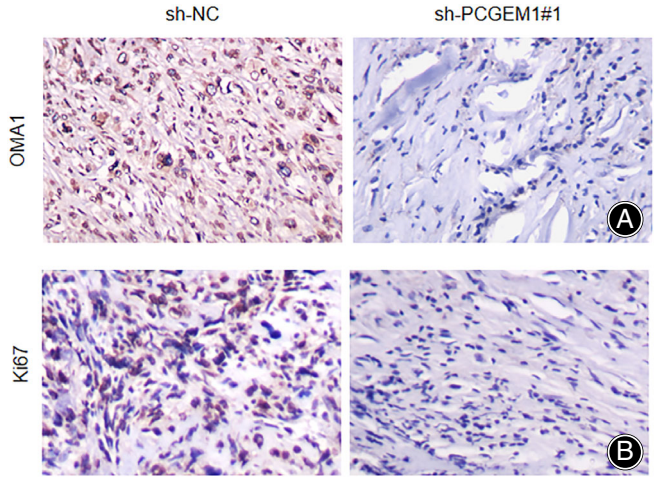

Fig. 6 Knockdown of PCGEM1 downregulates Ki67 and OMA1 expression in OS tumor. Positive expression of (A) Ki67 and (B) OMA1 in tumors of nude mice was detected by immunohistochemistry

Knockdown of PCGEM1 Downregulates Ki67 and OMA1 Expression in OS Tumor

As histological examination results showed (Fig. 6A,B), xenograft tumor comprised highly dense cancer cells with a pleomorphic spindle-shape characteristic of OS. Ki67 has been considered as a significant cellular marker of proliferation, and a decreased expression was observed in tumor specimens derived from sh-PCGEM1-treated group by immunohistochemical staining (Fig. 6A). And we also found that the OMA1 expression was suppressed in treated groups as well (Fig. 6B).

Discussion

Main Findings of this Study

OS is the most frequent primary bone sarcomas, and the highest incidence is in children and adolescents, while a second smaller peak of incidence lies in elderly individuals over 60 years.[27] We aimed at unveiling the potential of PCGEM1 as a biomarker for OS treatment. During our investigations, we showed the high expression of PCGEM1 in OS cells through RT-qPCR data. Then, the results of loss-of-function assays proved that knockdown of PCGEM1 in OS cells resulted in the repression of cell proliferation, migration, invasion, and EMT progression. Moreover, knockdown of PCGEM1 inhibited tumor growth and metastasis *in vivo*. Mechanistically, PCGEM1 functioned as a sponge for miR-433-3p to upregulate PCGEM1 expression. Additionally, overexpression of OMA1 reversed the PCGEM1 knockdown-mediated inhibitory effect on the malignant phenotype in OS cells. Accordingly, we concluded that PCGEM1 promotes OS progression through the miR-433-3p/PCGEM1 axis.

PCGEM1 in Cancer

A multitude of studies have suggested that lncRNAs are implicated in the regulation of a broad spectrum of cellular processes, such as proliferation, migration, and invasion.[28–30] PCGEM1 was utilized to be our research object. PCGEM1 has been widely reported to be an oncogenic gene in various cancers. PCGEM1 promotes renal carcinoma progression by targeting miR-433-3p to regulate FGF2 expression.[12] PCGEM1 contributes to malignant behaviors of glioma by regulating miR-539-5p/CDK6 axis.[31] PCGsEM1 contributes to the proliferation, migration, and invasion of non-small cell lung cancer cells *via* acting as a sponge for miR-152-3p.[32] In the current study, PCGEM1 showed a high expression in OS cells, suggesting that PCGEM1 may act as an oncogene in OS. Consistent with previous studies, functional assay revealed that the knockdown of PCGEM1 significantly suppressed cell proliferation, migration, invasion and EMT in OS. Finally, to explore the function of PCGEM1 *in vivo*, we constructed a xenograft tumor model in nude mice. We found that the inhibition of PCGEM1 suppressed tumor growth and metastasis of OS by decreasing tumor size, volume, weight, and lung metastasis *in vivo*. These results suggest that PCGEM1 may exert a key function as an oncogene in OS.

The ceRNA Regulatory Network in which PCGEM1 is Involved in OS

Mechanistically, lncRNAs act as ceRNAs by competitively binding with miRNAs to sequester these miRNAs, thereby modulating the levels of their downstream target genes.[33–35] In addition, such lncRNA/miRNA/mRNA ceRNA regulatory networks have been identified in several biological processes, including EMT, lung metastasis and chemo/radioresistance in OS.[36,37] MiRNAs are single-stranded RNAs without non-coding capacity and contain 22–24 nucleotides in length. Importantly, miRNAs could block the translation or degradation of target mRNAs to post-transcriptionally regulate gene expression.[38] Studies have revealed some miRNAs that participate in regulating OS progression and function as promising targets.[39,40] Although PCGEM1 has been widely reported to act as a ceRNA in cancer, the molecular mechanism of PCGEM1 in OS is still unknown. In the current study, we determined PCGEM1 subcellular distribution and found that PCGEM1was predominantly expressed in the cytoplasm of OS cells. This suggested the possibility that PCGEM1 could function as ceRNA *via* sponging miRNAs. Meanwhile, miR-433-3p was found to be a miRNA bearing the complementary base paring with PCGEM1. Previous research showed that miR-433-3p played a key role in OS progression.[41,42] Here, miR-485-5p expressed at a low level in OS cells and negatively associated with PCGEM1. Therefore, PCGEM1 acted as the molecular sponge of miR-433-3p in OS.

With the assistance of starBase, miR-433-3p was predicted and identified. Additionally, miR-433-3p was confirmed to bind to PCGEM1 with downregulated expression in OS. Hereafter, we further explored the target genes of miR-

433-3p, and OMA1 was selected, which has been proven to be a biomarker for several tumor treatments.[43,44] For example, OMA1 knockout suppresses colorectal cancer development and xenograft mice models of colorectal cancer.[45] Overexpression of OMA1 is potentially a biomarker and predicts an unfavorable prognosis in gastric cancer.[46] Here, we validated the interaction between miR-433-3p and OMA1 and revealed that the OMA1 level was positively regulated by PCGEM1 but negatively regulated by miR-433-3p. Rescue assays further verified that overexpression of OMA1 reversed the PCGEM1 knockdown-mediated inhibitory effect on the malignant phenotype including proliferation, migration, invasion and EMT in OS cells.

Limitations and Strengths of the Study

However, some limitations in this study are worth mentioning. First, it would be better to recruit clinical samples in subsequent experiments to enhance persuasion of our findings. Second, we would also conduct further research on some potential signaling pathways related to OS in a future study. However, our results may provide inspiration for further understanding of the mechanism of OS. We show that PCGEM1 might serve as a new target and biomarker for the treatment of OS.

Conclusion

In summary, we identified a novel OS-associated lncRNA PCGEM1. Through functional experiments, we illustrated that PCGEM1 was upregulated in OS; PCGEM1 upregulated OMA1 to promote OS cell proliferation, migration, and invasion by acting as a ceRNA that sponged miR-433-3p. In the future work, we will explore the mechanism of PCGEM1 upregulation in OS and the correlation between PCGEM1 and other miRNAs or proteins, which will further deepen our understanding of the pathogenesis of OS and make PCGEM1 a potential novel diagnostic and therapeutic target for OS.

Conflicts of Interest

The authors declare no conflict of interest.

Author Contributions

Jun Li conceived and designed the experiments. Jun Li, Yuanjin Zhang, Farui Sun, Guofu Zhang, Xi-an Pan, and Qian Zhou carried out the experiments. Jun Li and Qian Zhou analyzed the data. Jun Li and Qian Zhou drafted the manuscript. All authors agreed to be accountable for all aspects of the work. All authors have read and approved the final manuscript.

Ethical Approval

Animal experiments were reviewed and approved by the Institutional Animal Care and Use Committee of Wuhan Myhalic Biotechnology Co., Ltd.(approval number: 202109022).

References

1. Ritter J, Bielack SS. Osteosarcoma. Ann Oncol. 2010;21(Suppl 7): vii320–5.
2. Sweetnam R. Osteosarcoma. Ann R Coll Surg Engl. 1969;44(1):38–58.
3. Winkler K, Bielack S, Bieling P. Osteosarcoma. Curr Opin Oncol. 1990;2(3): 486–90.
4. Simpson E, Brown HL. Understanding osteosarcomas. Jaapa. 2018;31(8): 15–9.
5. Bielack SS, Kempf-Bielack B, Delling G, Exner GU, Flege S, Helmke K, et al. Prognostic factors in high-grade osteosarcoma of the extremities or trunk: an analysis of 1,702 patients treated on neoadjuvant cooperative osteosarcoma study group protocols. J Clin Oncol. 2002;20(3):776–90.
6. Jarroux J, Morillon A, Pinskaya M. History, discovery, and classification of lncRNAs. Adv Exp Med Biol. 2017;1008:1–46.
7. Xie Y, Zhang Y, du L, Jiang X, Yan S, Duan W, et al. Circulating long noncoding RNA act as potential novel biomarkers for diagnosis and prognosis of non-small cell lung cancer. Mol Oncol. 2018;12(5):648–58.
8. Jiang S, Cheng SJ, Ren LC, Wang Q, Kang YJ, Ding Y, et al. An expanded landscape of human long noncoding RNA. Nucleic Acids Res. 2019;47(15): 7842–56.
9. Wang G, Zhang ZJ, Jian WG, Liu PH, Xue W, Wang TD, et al. Novel long noncoding RNA OTUD6B-AS1 indicates poor prognosis and inhibits clear cell renal cell carcinoma proliferation via the Wnt/β-catenin signaling pathway. Mol Cancer. 2019;18(1):15.
10. Zhuo W, Liu Y, Li S, Guo D, Sun Q, Jin J, et al. Long noncoding RNA GMAN, up-regulated in gastric cancer tissues, is associated with metastasis in patients and promotes translation of ephrin A1 by competitively binding GMAN-AS. Gastroenterology. 2019;156(3):676–691.e11.
11. Srikantan V, Zou Z, Petrovics G, Xu L, Augustus M, Davis L, et al. PCGEM1, a prostate-specific gene, is overexpressed in prostate cancer. Proc Natl Acad Sci U S A. 2000;97(22):12216–21.
12. Cai X, Zhang X, Mo L, Zhu J, Yu H. LncRNA PCGEM1 promotes renal carcinoma progression by targeting miR-433-3p to regulate FGF2 expression. Cancer Biomark. 2020;27(4):493–504.
13. Li Q, Shen F, Zhao L. The relationship between lncRNA PCGEM1 and STAT3 during the occurrence and development of endometrial carcinoma. Biomed Pharmacother. 2018;107:918–28.
14. Weng L, Qiu K, Gao W, Shi C, Shu F. LncRNA PCGEM1 accelerates non-small cell lung cancer progression via sponging miR-433-3p to upregulate WTAP. BMC Pulm Med. 2020;20(1):213.
15. Zhang T, Piao HY, Guo S, Zhao Y, Wang Y, Zheng ZC, et al. LncRNA PCGEM1 enhances metastasis and gastric cancer invasion through targeting of miR-129-5p to regulate P4HA2 expression. Exp Mol Pathol. 2020;116:104487.
16. Xu Z, Meng L, Xie Y, Guo W. lncRNA PCGEM1 strengthens anti-inflammatory and lung protective effects of montelukast sodium in children with cough-variant asthma. Braz J Med Biol Res. 2020;53(7):e9271.
17. Zhao Y, Xu J. Synovial fluid-derived exosomal lncRNA PCGEM1 as biomarker for the different stages of osteoarthritis. Int Orthop. 2018;42(12):2865–72.
18. Chen J, Yuan D, Hao Q, Zhu D, Chen Z. LncRNA PCGEM1 mediates oxaliplatin resistance in hepatocellular carcinoma via miR-129-5p/ETV1 axis in vitro. Adv Clin Exp Med. 2021;30(8):831–8.
19. Petrovics G, Zhang W, Makarem M, Street JP, Connelly R, Sun L, et al. Elevated expression of PCGEM1, a prostate-specific gene with cell growth-promoting function, is associated with high-risk prostate cancer patients. Oncogene. 2004;23(2):605–11.
20. Lee YS, Dutta A. MicroRNAs in cancer. Annu Rev Pathol. 2009;4:199–227.
21. Ma R et al. miRNA-mRNA interaction network in non-small-cell lung cancer. Interdiscip Sci. 2015.
22. Zhang Q et al. Hypoxia-induced microRNA-10b-3p promotes esophageal squamous cell carcinoma growth and metastasis by targeting TSGA10. Aging. 2019;11(22):10374–84.
23. Schneider E et al. MicroRNA-708 is a novel regulator of the Hoxa9 program in myeloid cells. Leukemia. 2019;34(5):1253–65.
24. Shi Q, Wang Y, Mu Y, Wang X, Fan Q. MiR-433-3p inhibits proliferation and invasion of esophageal squamous cell carcinoma by targeting GRB2. Cell Physiol Biochem. 2018;46(5):2187–96.
25. Tang X, Lin J, Wang G, Lu J. MicroRNA-433-3p promotes osteoblast differentiation through targeting DKK1 expression. PLoS One. 2017;12(6): e0179860.
26. Tay Y, Rinn J, Pandolfi PJN. The multilayered complexity of ceRNA crosstalk and competition. 2014;505(7483):344–52.
27. Corre I et al. The osteosarcoma microenvironment: a complex but targetable ecosystem. Cell. 2020;9(4):976.

28. Quinn JJ, Chang HY. Unique features of long non-coding RNA biogenesis and function. Nat Rev Genet. 2016;17(1):47–62.
29. Leone S, Santoro R. Challenges in the analysis of long noncoding RNA functionality. FEBS Lett. 2016;590(15):2342–53.
30. Fang Y, Fullwood MJ. Roles, functions, and mechanisms of long non-coding RNAs in cancer. Genomics Proteomics Bioinformatics. 2016;14(1):42–54.
31. Liu SL, Chen MH, Wang XB, You RK, An XW, Zhao Q, et al. LncRNA PCGEM1 contributes to malignant behaviors of glioma by regulating miR-539-5p/CDK6 axis. Aging. 2021;13(4):5475–84.
32. Huang J, Lou J, Liu X, Xie Y. LncRNA PCGsEM1 contributes to the proliferation, migration and invasion of non-small cell lung cancer cells via acting as a sponge for miR-152-3p. Curr Pharm Des. 2021;27(46):4663–70.
33. Chan JJ, Tay Y. Noncoding RNA:RNA regulatory networks in cancer. Int J Mol Sci. 2018;19(5):1310.
34. Zhang R et al. Candidate lncRNA-miRNA-mRNA network in predicting hepatocarcinogenesis with cirrhosis: an integrated bioinformatics analysis. J Cancer Res Clin Oncol. 2019;146(1):87–96.
35. Zhou Y, Xu Z, Yu Y, Cao J, Qiao Y, Qiao H, et al. Comprehensive analysis of the lncRNA-associated ceRNA network identifies neuroinflammation biomarkers for Alzheimer's disease. Mol Omics. 2019;15(6):459–69.
36. Yu Y et al. Long noncoding RNA CRNDE functions as a diagnostic and prognostic biomarker in osteosarcoma, as well as promotes its progression via inhibition of miR-335-3p. J Biochem Mol Toxicol. 2021;35(5):e22734.
37. Wang L et al. Long noncoding RNA HCG9 promotes osteosarcoma progression through RAD51 by acting as a ceRNA of miR-34b-3p. Mediators Inflamm. 2021;2021:9978882.
38. Rupaimoole R, Slack FJ. MicroRNA therapeutics: towards a new era for the management of cancer and other diseases. Nat Rev Drug Discovery. 2017;16(3):203–22.
39. Geng Y, Zhao S, Jia Y, Xia G, Li H, Fang Z, et al. miR-95 promotes osteosarcoma growth by targeting SCNN1A. Oncol Rep. 2020;43(5):1429–36.
40. Gu Z, Wu S, Xu G, Wu W, Mao B, Zhao S. miR-487a performs oncogenic functions in osteosarcoma by targeting BTG2 mRNA. Acta Biochim Biophys Sin. 2020;52(6):631–7.
41. Hou XK, Mao JS. Long noncoding RNA SNHG14 promotes osteosarcoma progression via miR-433-3p/FBXO22 axis. Biochem Biophys Res Commun. 2020;523(3):766–72.
42. Zhang M, Yu GY, Liu G, Liu WD. Circular RNA circ_0002137 regulated the progression of osteosarcoma through regulating miR-433-3p/ IGF1R axis. J Cell Mol Med. 2022;26(6):1806–16.
43. Amini MA et al. Overexpression of ROMO1 and OMA1 are potentially biomarkers and predict unfavorable prognosis in gastric cancer. J Gastrointest Cancer. 2019;51(3):939–46.
44. Alavi MV. Targeted OMA1 therapies for cancer. Int J Cancer. 2019;145(9):2330–41.
45. Wu Z, Zuo M, Zeng L, Cui K, Liu B, Yan C, et al. OMA1 reprograms metabolism under hypoxia to promote colorectal cancer development. EMBO Rep. 2021;22(1):e50827.
46. Amini MA, Karimi J, Khodadadi I, Tavilani H, Talebi SS, Afshar B. Overexpression of ROMO1 and OMA1 are potentially biomarkers and predict unfavorable prognosis in gastric cancer. J Gastrointest Cancer. 2020;51(3):939–46.